Proc. Natl. Acad. Sci. USA
Vol. 84, pp. 104–108, January 1987
Botany

Blue-light reception in *Phycomyces* phototropism: Evidence for two photosystems operating in low- and high-intensity ranges

(blue-light photoreceptors/fluence rate–response relationships/action spectroscopy/sensory adaptation)

PAUL GALLAND AND EDWARD D. LIPSON*

Department of Physics, Syracuse University, Syracuse, NY 13244-1130

Communicated by Winslow R. Briggs, September 19, 1986 (received for review January 21, 1986)

ABSTRACT **Phototropism in the fungus *Phycomyces* is mediated by two photosystems that are optimized for the low-intensity region (below 10^{-6} W·m^{-2}) and the high-intensity region (above 10^{-6} W·m^{-2}). These photosystems can be distinguished under special experimental conditions, in which sporangiophores grown in the dark are suddenly exposed to continuous unilateral light. With this treatment, the bending occurs in two steps. Below 10^{-6} W·m^{-2}, an early-response component (15-min latency) and a late-response component (50- to 70-min latency) are observed that are mediated by photosystem I. Above 10^{-6} W·m^{-2}, the early component is augmented by an intermediate component with a 40-min delay that is mediated by photosystem II. The two photosystems are distinguished further by their wavelength sensitivities and adaptation kinetics. Photosystem I is more effective at 334, 347, and 550 nm than photosystem II, but it is less effective at 383 nm. At wavelength 450 nm, the dark-adaptation kinetics associated with photosystem I are approximately half as fast as those associated with photosystem II. However, the light-adaptation kinetics of photosystem I are ≈3 times faster than the kinetics associated with photosystem II. The existence of two photosystems clarifies several behavioral features of *Phycomyces* and helps explain how the sporangiophore can manage the full range of 10 decades.**

Blue light plays an important role in higher and lower plants and in numerous microorganisms (1). The giant sporangiophore (fruiting body) of the fungus *Phycomyces* bends toward unilateral blue light (phototropism) and modulates its elongation rate transiently after changes of ambient light intensity (light-growth response) (2). The receptor pigment(s) (cryptochromes) that operate in *Phycomyces* and in other blue-light-sensitive organisms have yet to be isolated and identified (1, 3). Organisms with cryptochrome photoreceptors typically have action spectra with major peaks around wavelengths of 450 and 480 nm, a smaller peak around 370 nm, and a sharp fall-off beyond 510 nm. In *Phycomyces*, evidence from action spectroscopy (4, 5), genetics (6), and studies with riboflavin analogs (7) suggests that flavoproteins are the most likely receptor pigment candidates.

Phototropism and the related light growth response in *Phycomyces* operate over an enormous intensity range, from 10^{-9} to 10 W·m^{-2} (2). Efficient light- and dark-adaptation processes are needed to provide range adjustment of sensitivity as the ambient intensity changes. A large sensitivity range is a feature of phototropism common among several organisms. The *Avena* (oat) coleoptile, the most extensively studied model system for phototropism in higher plants, spans a range of ≈10^6:1 (8). How the phototropic photosystems of these organisms can manage such large ranges is unknown. One possibility is that these blue-light-sensitive organisms have several photosystems for different intensity regions.

We present experimental evidence that strongly supports the existence of two photosystems in *Phycomyces* phototropism. These findings may apply to other blue-light-sensitive organisms, especially those that show similar phototropic behavior.

MATERIALS AND METHODS

Culture Conditions. The standard wild-type strain NRRL1555 of *Phycomyces blakesleeanus* Burgeff was used in this work. Sporangiophores were grown in shell vials (diameter, 10 mm; height, 35 mm) containing 4% potato dextrose agar (Difco) and 0.5 μg of vitamin B-1 per ml (thiamine hydrochloride; Sigma). Each vial was inoculated with an average of five heat-shocked spores (48°C for 10 min). After inoculation, the vials were kept in a temperature-controlled darkroom at 20°C under red safelight (9×10^{-3} W·m^{-2}). Two days after inoculation and before the development of sporangiophores, the vials were transferred to a dark cabinet. This cabinet and the experimental phototropism chambers were located in the same temperature-controlled room.

Phototropism Experiments. Sporangiophores were left in the dark cabinet for ≈50 hr until they reached stage IVb, which is characterized by a mature black sporangium and steady growth rate (2). In this developmental stage, the sporangiophores typically had a height of 2–2.5 cm and growth rates of 2–3 mm/hr. They were transferred under red safelight to specially designed phototropism chambers and were then allowed to adapt for 30 min to the new environment before the experiments began. A detailed description of the phototropism chambers, the light sources, the calibration procedures, and the video recording techniques has been presented elsewhere (9, 10). Filter holders on the phototropism chambers each contained a heat-absorbing filter (type KG-1; Schott Optical Glass, Duryea, PA), interference filters (Balzers, obtained from Rolyn Optics, Covina, CA; bandwidth, 9–12 nm), and neutral-density filters (type NG; Schott). For experiments at wavelength 347 nm, an additional near-ultraviolet bandpass filter was used (type UG11; Schott).

RESULTS

Phototropism of Dark-Adapted Sporangiophores. Phototropism of *Phycomyces* sporangiophores has usually been studied under conditions where the bending response is continuous. When light-grown light-adapted sporangiophores are exposed to continuous unilateral light, they bend toward the light source continuously, without interruption. After an initial latent period of several minutes, the bending rate

The publication costs of this article were defrayed in part by page charge payment. This article must therefore be hereby marked "*advertisement*" in accordance with 18 U.S.C. §1734 solely to indicate this fact.

*To whom reprint requests should be addressed.

remains nearly constant until an equilibrium angle is reached where the negative gravitropic stimulus balances the positive phototropic stimulus (2, 6, 10, 11). This angle is called the photogravitropic equilibrium angle. A typical bending response of this type is shown in Fig. 1*B* (dashed line).

We discovered that dark-grown dark-adapted sporangiophores behave quite differently. While they are exposed to continuous unilateral light, such sporangiophores bend toward the light source in two distinct steps. Typical responses are shown in Fig. 1. After the unilateral light is switched on, bending begins after a latency time (t_1) (Fig. 1*A*) of ≈15 min and continues for <30 min. After a latency time (t_2) (Fig. 1*A*), bending resumes until a photogravitropic equilibrium angle α_2 is reached. The latency t_2 (or t_3 in Fig. 1*B*) is determined by extrapolating the linear portion of the bending curve back to the plateau value of α_1. Extrapolation to zero response of the second component is impossible, because the extrapolation of the late component with its typically shallow slope often intersects the abscissa before zero time. The apparent extrapolation of both the intermediate and the late component in Fig. 1 to ≈40 min is fortuitous. Three components of the bending response were found: (*i*) an early component with a latency t_1 of ≈15 min and moderate bending rates between 1 and 3 deg·min^{-1}, (*ii*) an intermediate component with a latency t_2 of 35–40 min and bending rates reaching 4 deg·min^{-1}, and (*iii*) a late component with a latency t_3 of 50–70 min and bending rates of ≈1 deg·min^{-1}.

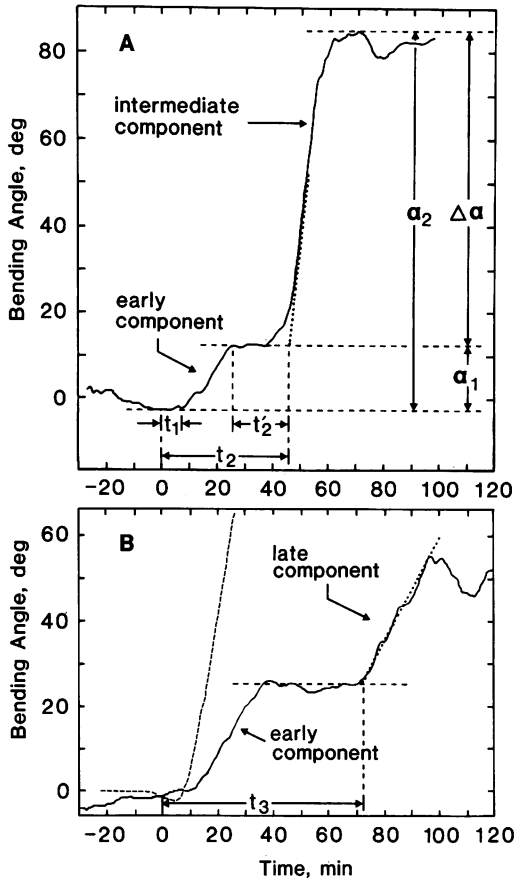

FIG. 1. Phototropic responses of dark-grown dark-adapted sporangiophores to continuous unilateral light of wavelength 452 nm. The light was switched on at time $t = 0$. The video camera was perpendicular to the stimulus beam so that the recorded bending angle was obtained from the projection of the sporangiophore onto the vertical plane containing the lamp. (*A*) Fluence rate = 7×10^{-4} W·m^{-2}. Definition of variables: t_1 = phototropic latency of early response component; t_2 = phototropic latency of the intermediate response component; t_2' = time between end of early response component and beginning of following response component (here the intermediate response component); α_2 = total maximal bending angle; α_1 = maximal bending angle of the early response component; $\Delta\alpha = (\alpha_2 - \alpha_1)$ = maximal bending angle of the intermediate or late response component. (*B*) Solid line, fluence rate = 1.2×10^{-8} W·m^{-2}; t_3 = phototropic latency of the late response component. Dashed line, light-adapted sporangiophore; the specimen was rotated for 40 min at 7×10^{-4} W·m^{-2} and then rotation was stopped at time $t = 0$.

Fluence Rate–Response Curves. For each of the three response components defined above, we analyzed both the bending angle and the bending rate and also the phototropic latency as a function of the fluence rate (Fig. 2). The bending rate and the phototropic latency t_1 of the early component are shown in Fig. 2*A*. The bending rate shows a maximum of 3 deg·min^{-1} in the low-intensity range at 1.5×10^{-8} W·m^{-2}. At most intensities, the latency is less than 16–18 min. It is this short latency that defines the early component. The maximal bending angle α_1 (Fig. 2*B*) has a pair of maxima below 10^{-6} W·m^{-2}. Fig. 2 *A* and *B* shows that the early component occurs over the entire intensity range from 10^{-9} to 1 W·m^{-2}.

The intermediate component, characterized by latencies t_2 of 35–40 min, occurs only above 10^{-6} W·m^{-2} (Fig. 2 *C* and *D*). In the high-intensity range between 10^{-4} and 10^{-3} W·m^{-2}, the bending rate for this component reaches a maximum of 5 deg·min^{-1}. The maximal bending angle $\Delta\alpha$ has a broad optimum around 10^{-3} W·m^{-2}.

The late component, characterized by latencies t_3 of 50–70 min and moderate bending rates (<1 deg·min^{-1}), occurs only below 10^{-6} W·m^{-2} (Fig. 2 *E* and *F*). The associated maximal bending angle $\Delta\alpha$ reaches a maximum of ≈30 deg around 10^{-7} W·m^{-2}. Thus, the dependence of the late component on low intensity distinguishes it from the intermediate component. The intermediate and late components can be distinguished also by the delay t_2' (defined in Fig. 1*A*), which is the time that elapses between the end of the early-response component and the beginning of the following component (intermediate or late). Fig. 2*G* shows that t_2' abruptly decreases from 40 to 15 min near 10^{-6} W·m^{-2}—i.e., at the threshold value for the intermediate component. We could not determine whether the late component is also present above 10^{-6} W·m^{-2}, because, by the time the late-response component began (50–70 min after the unilateral light was switched on), the early component and, even more so, the intermediate component with its increased bending rate would have masked any contribution of the rather inefficient late component. Thus, we could not define the entire intensity range for the late component, but only the lower range.

To see whether the two-step bending was really caused by the sudden dark-to-light transition, rather than by the absolute intensity alone, we performed control experiments with light-adapted sporangiophores over the entire intensity range. Sporangiophores were exposed to unilateral light for 1 hr while they were rotated around their axis to avoid bending. Rotation was then stopped so that the light was applied unilaterally. Below 1.2×10^{-8} W·m^{-2}, we usually found (data not shown) two-step phototropism as in Fig. 1*B* (solid line). At all other intensities, bending occurred in one continuous response as shown in Fig. 1*B* (dashed line).

The occurrence of different phototropic latencies and the shapes of the fluence rate-response curves suggest the presence of two photosystems. We propose that two photosystems control the three response components: a low-intensity photosystem (designated as photosystem I) mediates the early and late components, and a high-intensity photosystem (photosystem II) mediates the intermediate component. The experiments described below were done to test this hypothesis.

Action Spectroscopy. Further support for the existence of two photosystems could be provided if they showed distinct wavelength sensitivities (action spectra). We therefore mea-

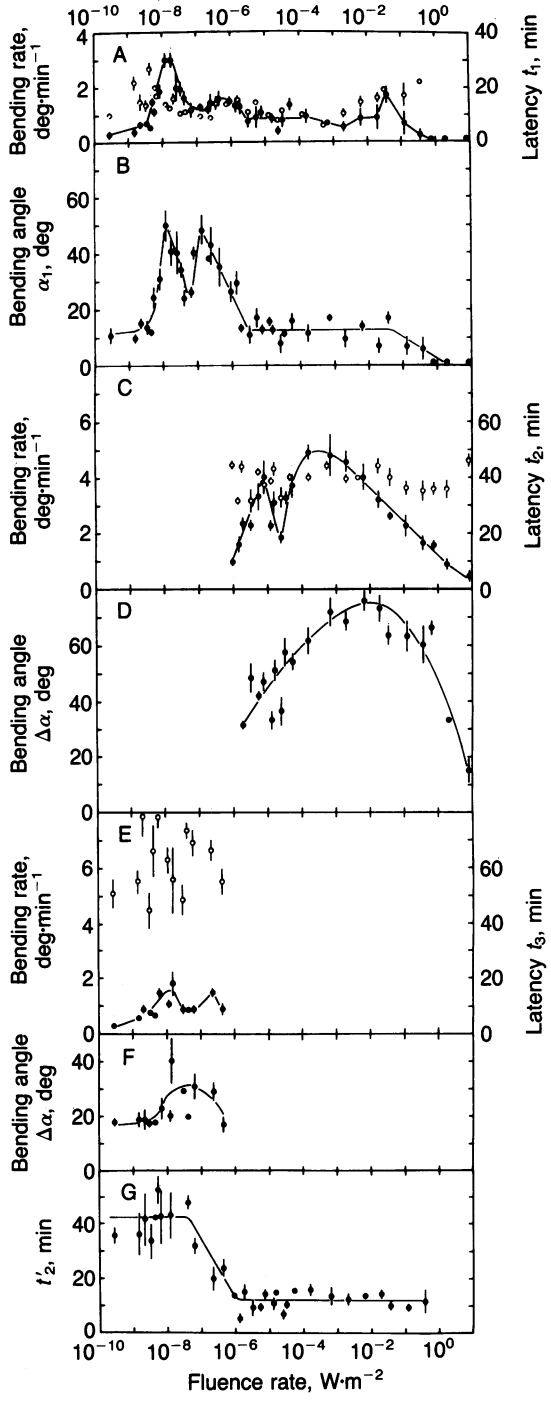

FIG. 2. Fluence rate–response curves (wavelength 452 nm) for phototropism of dark-grown dark-adapted sporangiophores. The experiments and measurements were done as described in *Materials and Methods* and Fig. 1. Error bars in this and the following figures represent the SEM of at least six experiments. (*A*) Early response component. ●, Bending rate; ○, phototropic latency t_1. (*B*) Early response component. Maximal bending angle α_1. (*C*) Intermediate response component. ●, Bending rate; ○, phototropic latency t_2. (*D*) Intermediate response component. Maximal bending angle $\Delta\alpha$. (*E*) Late response component. ●, Bending rate; ○, phototropic latency t_3. (*F*) Late response component. Maximal bending angle $\Delta\alpha$. (*G*) Delay t'_2, the time that elapses between the end of the early response component and the beginning of the following response component (intermediate or late).

sured partial action spectra for the three response components by first obtaining fluence rate–response curves (like those shown in Fig. 2) at five wavelengths: 334, 347, 383, 450, and 550 nm. For each response component, we then calculated the relative quantum efficiency at these wavelengths with respect to the 450-nm reference wavelength. Fig. 3 shows the action spectra for the bending rate. They were obtained from fluence rate–response curves like those shown in Fig. 2 *A* and *C*. The partial action spectra in Fig. 3 demonstrate that the two photosystems have distinct wavelength sensitivities. Photosystem II (intermediate-response component) has 5 times higher relative quantum efficiency at 383 nm than photosystem I (early-response component). By contrast, at 334, 347, and 550 nm, the respective quantum efficiencies of photosystem I are, respectively, 200, 5, and 10 times higher than those of photosystem II. These results support the hypothesis that two photosystems with distinct receptor pigments operate in the low- and high-intensity ranges. The partial action spectra for the bending angle (obtained from fluence rate–response curves of the type shown in Fig. 2 *B* and *D*) had a shape similar to those in Fig. 3 (data not shown).

Dark-Adaptation Kinetics. To obtain still more evidence for separate photosystems, we measured the phototropic dark-adaptation kinetics in the low- and the high-intensity ranges. These experiments were motivated by our previous finding that the dark-adaptation kinetics are mediated at the photoreceptor level (10, 11). If we could detect different adaptation kinetics in the low- and high-intensity ranges, this too would indicate that different photosystems operate at these intensities.

In our phototropic dark adaptation experiments (Fig. 4), symmetrically light-adapted sporangiophores were suddenly exposed to unilateral light of lower intensity. The phototropic latency was measured as a function of the unilateral intensity (note the reversal of axes in Fig. 4, so that the dependent variable is shown on the abscissa to portray more clearly the time dependence of adaptation). Dark-grown sporangiophores were first light-adapted (450-nm wavelength) for 60 min at 4.6×10^{-7} or 6.4×10^{-3} W·m^{-2} (the uppermost points of the two curves in Fig. 4), while they were rotated around

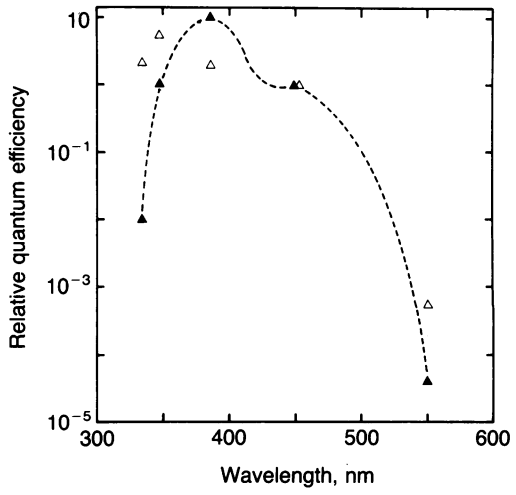

FIG. 3. Partial action spectrum for the phototropic bending rate mediated by photosystem I (early-response component; low-intensity range) and photosystem II (intermediate-response component; high-intensity range). For each wavelength, photon fluence–response curves (expressed as mol of photons per m^2·sec) of the type shown in Fig. 2 *A* and *C* were measured. The relative quantum effectiveness Φ at wavelength λ compared to wavelength 450 nm was calculated as $\Phi = I_{450}/I_\lambda$, where I_{450} is the photon fluence rate at 450 nm to elicit a criterion response and I_λ is the photon fluence rate at wavelength λ to elicit the same response. Δ, Photosystem I; relative quantum effectiveness was calculated for the absolute threshold (extrapolation to zero response). ▲, Photosystem II; relative quantum effectiveness was calculated for criterion response of 1 deg·min^{-1}.

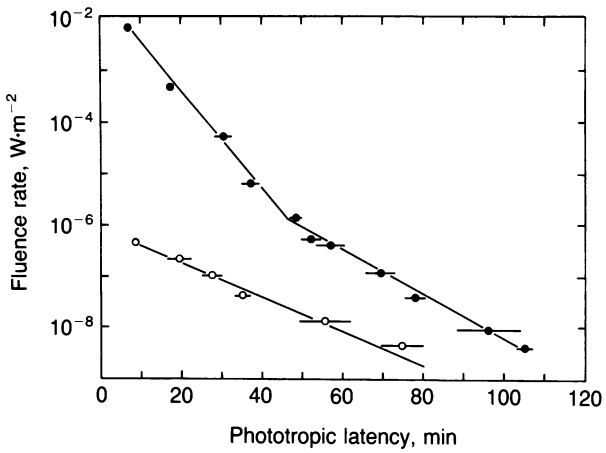

FIG. 4. Phototropic dark-adaptation kinetics at wavelength 450 nm. Upper curve (●), dark-grown sporangiophores were light-adapted for 1 hr at 6.4×10^{-3} W·m^{-2} (the uppermost data point of the curve) while they were rotated around their vertical axes to obviate bending. Then the light intensity (fluence rate) was stepped down to the level indicated on the ordinate and rotation was stopped, so that the light was applied unilaterally. The phototropic latency given on the abscissa was determined as described in the text. Lower curve (○), same procedure as described above. Dark-grown sporangiophores were light adapted for 1 hr at 4.6×10^{-7} W·m^{-2} while they were rotated. At time zero, the rotation was stopped and unilateral light of reduced intensity was given. Error bars represent SEM of at least six experiments. The curves are nonlinear least-squares fits to the function $A = A_1 \exp[-(t - t_0)/b_1] + (I - A_1) \exp[-(t - t_0)/b_2]$, where I is the intensity to which the sporangiophore is adapted, t_0 is the intrinsic latency for experiments involving no step down of intensity, and b_1 and b_2 are the time constants of dark adaptation. This equation was solved implicitly for t as a function of A during the least-squares fitting procedure.

their vertical axes, so that no bending would occur during the period of light adaptation. Then, after the rotation was stopped and the intensity was reduced (both at $t = 0$), the bending response was measured and plotted as in Fig. 1*B* (dashed line). To obtain the phototropic latency, the linear part of each bending curve was extrapolated to zero degrees bending (t_1 in Fig. 1*A*); the phototropic latency was defined as the time of the intercept between the extrapolated curve and the abscissa. As reported earlier (10, 11), only one response component is observed in such experiments with light-adapted sporangiophores.

Fig. 4 shows that the phototropic latency increases progressively for larger steps down of intensity. The crucial feature of this dark-adaptation behavior is that the kinetics obtained in the high-intensity range between 6.4×10^{-3} and 10^{-6} W·m^{-2} are over twice as fast as those measured in the low-intensity range between 4.6×10^{-7} and 10^{-9} W·m^{-2}. Below 10^{-6} W·m^{-2}, the dark-adaptation kinetics are slow regardless of whether the sporangiophore had been preadapted in the high-intensity region (upper curve) or the low-intensity region (lower curve).

For sporangiophores preadapted at 4.6×10^{-7} W·m^{-2}, the single time constant is $b = 12.3 \pm 0.5$ min; for sporangiophores preadapted at 6.4×10^{-3} W·m^{-2}, the second time constant (for the data below 10^{-6} W·m^{-2}) is $b_2 = 10.9 \pm 0.8$ min. Sporangiophores that were preadapted at 6.4×10^{-3} W·m^{-2} start with rapid kinetics ($b_1 = 4.3 \pm 0.2$ min) that become about half as fast below 10^{-6} W·m^{-2}. The essential feature of these biphasic kinetics is that the break of the curve coincides with the threshold region of photosystem II. This indicates that the fast dark-adaptation kinetics are associated with photosystem II, and the slow dark-adaptation kinetics are associated with photosystem I. Other specimens that were preadapted at 3.6×10^{-4} or 1 W·m^{-2} also had a fast monophasic dark-adaptation kinetics in the high-intensity range (data not shown). The observation of different kinetics in the low- and high-intensity ranges reinforces our conclusion that separate photosystems are operating in these two ranges.

Assuming that light adaptation, like dark adaptation, is a first-order process, we estimated the time constants for the light-adaptation kinetics from the latencies of the early and intermediate response components. This estimate can be made in the framework of the Delbrück–Reichardt model of adaptation (12). According to their model, the adaptation level A reaches the new intensity level I according to the relationship

$$A = A_0 + (I - A_0)\,[1 - \exp(-t/b)], \qquad [1]$$

where A_0 is the adaptation level before the step up to intensity I, t is the time, and b is the time constant of light adaptation. For light-grown light-adapted sporangiophores, this relationship describes the time course of light adaptation as long as moderate light steps are applied (11). The time required for A to reach the new intensity level depends mainly on the ratio of t to b and is almost independent of $(I - A_0)$. This means that the time to adapt to the new intensity is independent of the intensity step up provided that the adaptation mechanism cannot resolve a difference $(I - A)$ smaller than 5% of $(I - A_0)$, as has been shown to be the case (11). The phototropic latencies associated with the early bending component and the intermediate bending component are almost independent of the intensity steps up ($\approx$15 min and $\approx$40 min, respectively). Thus, one can apply Eq. **1** to estimate the time constants of light adaptation without actually measuring the kinetics (as we had to do in the case of dark adaptation). For photosystem I (early component), one obtains a time constant of $b \cong 5$ min and for photosystem II (intermediate component), a time constant of $b \cong 13$ min. Thus, photosystem I exhibits slow dark adaptation and fast light adaptation. Conversely, in photosystem II, dark adaptation is rapid and light adaptation is slow.

DISCUSSION

Our data indicate that two photosystems operate in *Phycomyces* phototropism. These photosystems can be distinguished by (*i*) the intensity ranges for which they are optimized, (*ii*) phototropic latencies, (*iii*) wavelength sensitivities, and (*iv*) time constants for adaptation. The presence of different photosystems helps explain how the sporangiophore photoresponses in *Phycomyces* can span the prodigious intensity range of 10^{10}:1. Our results strengthen our previous conclusions (3, 10, 13) that three major functions of the sensory transduction chain—i.e., intensity discrimination, wavelength discrimination, and sensory adaptation—are all processed at the level of the photoreceptor system.

We were able to distinguish the two photosystems, because we could resolve several bending components with distinct latencies. This stepwise behavior is obtained only for dark-grown dark-adapted sporangiophores after exposure to continuous unilateral light. Light-grown light-adapted sporangiophores and dark-grown light-adapted sporangiophores always exhibit short phototropic latencies of 6–10 min when exposed to unilateral light (11, 14).

In the past few years, considerable evidence has accumulated that the photoreceptor system of the *Phycomyces* sporangiophore is complex and contains more than a single photoreceptor pigment (5, 10, 15–17). The results presented here strengthen and considerably enlarge the multiphotoreceptor concept because they allow us now to attribute specific intensity ranges, wavelength sensitivities, and kinetic properties to the two photosystems. It remains to be

determined whether each photosystem consists of a single receptor pigment, several receptor pigments, a photochromic pigment, or a photocycling pigment. There are already clear indications that both photosystems are complex and that each contains more than just a single receptor pigment. For photosystem I, support for this conclusion comes from the following observations: (*i*) complex fluence rate–response curves for the bending rate and bending angle (Fig. 2 *A–C*), (*ii*) failure of the reciprocity rule for millisecond pulses given at threshold fluences (13), (*iii*) antagonistic interaction between blue and near-ultraviolet light just above threshold (5), and (*iv*) antagonistic interaction between continual dichromatic pulses (red–blue) or monochromatic (blue–blue) pulses in photogravitropic equilibrium experiments (16, 17). The complex shape of the fluence rate–response curves for the bending rate in the high-intensity range (Fig. 2*C*) indicates that photosystem II also has more than one receptor pigment.

The finding of distinct photosystems has an important bearing on the interpretation of phototropism action spectra. It was discovered recently in *Phycomyces* that the shapes of these action spectra depend critically on the methods by which they are measured (5, 15, 18). An action spectrum of photogravitropic equilibrium measured near threshold with monochromatic irradiation shows a prominent peak in the near-ultraviolet spectrum (15). The relative quantum efficiency at 386 nm is similar to that at 450 nm (15, 18, 19). Our partial action spectra (Fig. 3) for the early and late components similarly have high quantum efficiencies at 386 nm. If, however, the action spectrum is measured near threshold with the phototropic balance method (balancing the sporangiophore between a test light at one of several wavelengths and variable intensity, and a reference light at wavelength 450 nm and fixed intensity), then the relative quantum efficiency at 386 nm is reduced to ≈10% of that at 450 nm (4). The 450-nm light evidently antagonizes the action of the near-ultraviolet light. Because this antagonism occurs near threshold—i.e., far below the intensity range of photosystem II—we infer that photosystem I itself must be complex.

In phototropic balance experiments in the high-intensity range at 0.1 $W \cdot m^{-2}$, the quantum effectiveness at 386 nm relative to 450 nm is 1.3 (4). This enhancement in the near-ultraviolet region is most likely due to the contribution of photosystem II with its enhanced sensitivity to 383-nm light. It appears that the antagonistic action between blue and 383-nm light is restricted to the low-intensity region. This does not preclude the possibility of photoreceptor antagonism in the high-intensity range. It should, however, be of a different type than the antagonism found in the low-intensity range.

Experimental evidence for a flavin photoreceptor in *Phycomyces* phototropism was provided by the observation that roseoflavin, a flavin analog with a bathochromic shift, was able to replace the endogenous photoreceptor and cause a corresponding shift in the phototropic balance action spectrum (7). These experiments were done near the phototropic threshold. The conclusions from these experiments therefore apply to photosystem I, but not necessarily to photosystem II.

Our data on dark-grown sporangiophores offer insight into the process of sensory adaptation. The dark adaptation kinetics (Fig. 4) are first order (single exponential), provided that the light intensity remains within the operating range of either photosystem. These results agree very well with the adaptation model proposed by Delbrück and Reichardt (12). Their model predicts furthermore that the phototropic latencies, after increasing steps up in light intensity, remain essentially constant; for example, the latency should be nearly identical for steps up by factors of 10 or 10,000. An important result of our experiments is that the phototropic latencies of the early and intermediate response components are indeed independent of the magnitude of the step up in light intensity. The explanation is that each photosystem has a distinct light-adaptation time constant and therefore a distinct phototropic latency in response to a step up. Thus, each photosystem seems to function according to the Delbrück–Reichardt model of adaptation. In previous phototropism experiments with light-grown sporangiophores (11), the contributions of separate photosystems could not be recognized (because the response did not occur stepwise; see above), and thus the Delbrück–Reichardt model sometimes appeared to be violated (10, 11, 20).

Finally, our findings may be of general relevance to other blue-light-sensitive systems such as *Avena* or *Zea* coleoptiles. *Phycomyces*, a lower fungus, shares with these plant systems a number of features, including cryptochrome action spectra (4, 21) and complex fluence–response curves with two maxima (first and second phototropic curvatures) (8, 13, 22, 23). The entire intensity range of these organisms is also large enough that one might expect separate photosystems to operate in different intensity ranges.

This work was supported by Grant GM29707 from the National Institutes of Health to E.D.L.

1. Senger, H. (1984) *Blue Light Effects in Biological Systems* (Springer, Berlin).
2. Russo, V. E. A. & Galland, P. (1980) *Struct. Bonding (Berlin)* **41**, 71–110.
3. Galland, P. & Lipson, E. D. (1984) *Photochem. Photobiol.* **40**, 795–800.
4. Delbrück, M. & Shropshire, W., Jr. (1960) *Plant Physiol.* **35**, 194–204.
5. Galland, P. & Lipson, E. D. (1985) *Photochem. Photobiol.* **41**, 323–329.
6. Presti, D., Hsu, W. J. & Delbrück, M. (1977) *Photochem. Photobiol.* **26**, 403–405.
7. Otto, M. K., Jayaram, M., Hamilton, R. M. & Delbrück, M. (1981) *Proc. Natl. Acad. Sci. USA* **78**, 266–269.
8. Zimmermann, B. K. & Briggs, W. R. (1963) *Plant Physiol.* **38**, 248–253.
9. Lipson, E. D. & Häder, D.-P. (1984) *Photochem. Photobiol.* **39**, 437–441.
10. Galland, P., Pandya, A. & Lipson, E. D. (1984) *J. Gen. Physiol.* **84**, 739–751.
11. Galland, P. & Russo, V. E. A. (1984) *J. Gen. Physiol.* **84**, 101–118.
12. Delbrück, M. & Reichardt, W. (1956) in *Cellular Mechanisms in Differentiation and Growth*, ed. Rudnick, D. (Princeton Univ. Press, Princeton, NJ), pp. 3–43.
13. Galland, P., Palit, A. & Lipson, E. D. (1985) *Planta* **165**, 538–547.
14. Galland, P. & Russo, V. E. A. (1984) *J. Gen. Physiol.* **84**, 119–132.
15. Galland, P. & Lipson, E. D. (1985) *Photochem. Photobiol.* **41**, 331–335.
16. Löser, G. & Schäfer, E. (1984) in *Blue Light Effects in Biological Systems*, ed. Senger, H. (Springer, Berlin), pp. 118–123.
17. Schäfer, E., Löser, G. & Heim, B. (1983) *Ber. Deutsch. Bot. Ges.* **96**, 497–509.
18. Galland, P. (1983) *Photochem. Photobiol.* **37**, 221–228.
19. Varjú, D., Edgar, L. & Delbrück, M. (1961) *J. Gen. Physiol.* **45**, 47–58.
20. Lipson, E. D. & Block, S. M. (1983) *J. Gen. Physiol.* **81**, 845–859.
21. Shropshire, W., Jr., & Withrow, R. B. (1958) *Plant Physiol.* **33**, 360–365.
22. Briggs, W. R. (1960) *Plant Physiol.* **35**, 951–962.
23. Ino, M. & Schäfer, E. (1984) *Proc. Natl. Acad. Sci. USA* **81**, 7103–7107.